

Structural origins of relaxor behavior in a $0.96 (\text{Bi } 1/2 \text{ Na } 1/2) \text{TiO}_3 - 0.04 \text{BaTiO}_3$ single crystal under electric field

John E. Daniels, Wook Jo, Jürgen Rödel, Daniel Rytz, and Wolfgang Donner

Citation: *Applied Physics Letters* **98**, 252904 (2011); doi: 10.1063/1.3602316

View online: <http://dx.doi.org/10.1063/1.3602316>

View Table of Contents: <http://scitation.aip.org/content/aip/journal/apl/98/25?ver=pdfcov>

Published by the [AIP Publishing](#)

Articles you may be interested in

Structural stability and depolarization of manganese-doped $(\text{Bi}_{0.5}\text{Na}_{0.5})_{1-x}\text{Ba}_x\text{TiO}_3$ relaxor ferroelectrics
J. Appl. Phys. **116**, 154101 (2014); 10.1063/1.4898322

Anisotropy of ferroelectric behavior of $(1-x)\text{Bi}_{1/2}\text{Na}_{1/2}\text{TiO}_3-x\text{BaTiO}_3$ single crystals across the morphotropic phase boundary

J. Appl. Phys. **116**, 044111 (2014); 10.1063/1.4891529

Electric-field–temperature phase diagram of the ferroelectric relaxor system $(1-x)\text{Bi}_{1/2}\text{Na}_{1/2}\text{TiO}_3-x\text{BaTiO}_3$ doped with manganese

J. Appl. Phys. **115**, 194104 (2014); 10.1063/1.4876746

Electric-field-induced and spontaneous relaxor-ferroelectric phase transitions in $(\text{Na}_{1/2}\text{Bi}_{1/2})_{1-x}\text{Ba}_x\text{TiO}_3$

J. Appl. Phys. **112**, 124106 (2012); 10.1063/1.4770326

Observing the superparaelectric limit of relaxor $(\text{Na } 1/2 \text{ Bi } 1/2) 0.9 \text{Ba } 0.1 \text{TiO}_3$ nanocrystals

Appl. Phys. Lett. **89**, 112901 (2006); 10.1063/1.2337880

The advertisement features a blue background with a film strip on the left side. The text is in white and orange. The Oxford Instruments logo is in the bottom right corner.

Not all AFMs are created equal
Asylum Research Cypher™ AFMs
There's no other AFM like Cypher

www.AsylumResearch.com/NoOtherAFMLikeIt

OXFORD
INSTRUMENTS
The Business of Science®

Structural origins of relaxor behavior in a $0.96(\text{Bi}_{1/2}\text{Na}_{1/2})\text{TiO}_3-0.04\text{BaTiO}_3$ single crystal under electric field

John E. Daniels,^{1,a)} Wook Jo,² Jürgen Rödel,² Daniel Rytz,³ and Wolfgang Donner²

¹*School of Materials Science and Engineering, University of New South Wales, Sydney 2052, Australia*

²*Institute of Materials Science, Technische Universität Darmstadt, Petersenstr. 23, Darmstadt 64287, Germany*

³*FEE GmbH, Struthstr. 2, Idar-Oberstein 55743, Germany*

(Received 7 March 2011; accepted 2 June 2011; published online 24 June 2011)

Diffuse x-ray scattering intensities from a single crystal of $0.96(\text{Bi}_{1/2}\text{Na}_{1/2})\text{TiO}_3-0.04(\text{BaTiO}_3)$ have been collected at room temperature with and without application of an electric field along the [100] direction. Distinct features in the diffuse scattering intensities indicate correlations on a nanometer length scale. It is shown that locally correlated planar-like structures and octahedral tilt-domains within the room temperature rhombohedral R3c phase are both electrically active and are irreversibly affected by application of an electric field of 4.3 kV/mm. The field dependence of these nanoscale structures is correlated with the relaxor behavior of the material by macroscopic permittivity measurements. © 2011 American Institute of Physics. [doi:10.1063/1.3602316]

Lead-free electromechanical materials are attracting significant attention due to their potential as “environmentally friendly” alternatives to common commercial piezoelectric materials, such as lead zirconate titanate.¹ Recently, it has been shown that solid solutions of $(1-x)\text{Bi}_{1/2}\text{Na}_{1/2}\text{TiO}_3-(x)\text{BaTiO}_3$ (BNT-100xBT) contain a morphotropic phase boundary, where the electromechanical properties of the material are enhanced.¹⁻⁴ BNT-based materials are also categorized as relaxor materials, i.e., their dielectric response is frequency-dependent and linked to local structural fluctuations [polar nanoregions (PNRs)].^{5,6} The two main electrically active phases in the vicinity of the morphotropic phase boundary have been identified as R3c and P4bm.^{4,7-9}

In this letter, we present a single crystal diffuse x-ray scattering study on BNT-4BT; a concentration outside the morphotropic phase region that displays relaxor behavior. We show that nanoscale octahedral tilt domains are one source of the relaxor behavior of BNT-BT. We further argue that octahedral tilt domains are directly linked to local correlated atomic displacements, which have previously been attributed to structures analogous to Guinier–Preston zones (GPZs) in metals.^{10,11}

A BNT-4BT single crystal was prepared by top-seeded solution growth. The composition of the crystal (BNT-4BT) was determined by inductively coupled plasma optical emission spectroscopy. The crystal for x-ray measurements was cut using a high-precision diamond saw to a final size of $1.3 \times 1 \times 1 \text{ mm}^3$. The crystal orientation was such that silver paint electrodes were applied to two opposing (100) type faces. Scattering experiments were carried out at beamline ID15B of the European Synchrotron Radiation Facility. A beam energy of 87.6 keV was generated by a single Laue Si(511) monochromator. The beam size was set to $300 \times 300 \text{ }\mu\text{m}^2$ just prior to the sample using tungsten slits; the gauge volume sampled therefore contains approximately 0.5 g of material. The sample was mounted in a specifically

designed electric field chamber.¹² Diffraction intensities were collected in the forward direction using an x-ray image intensifier coupled to a charge coupled device camera. Images were collected over 100° of rotation around an axis perpendicular to the beam direction in 0.2° steps. Data were then rebinned into three-dimensional reciprocal space coordinates for interpretation. The dielectric permittivity of both poled and unpoled crystals were measured along the $[100]_{\text{pc}}$ orientation of platelet shape samples using an impedance spectroscopy (HP4192A). The d_{33} value of the crystal was measured to be 140 pC/N using a Berlincourt meter (YE 2730, Sinocera) after poling at 6 kV/mm for 1 min.

Figure 1(a) shows the reconstructed (hk0) plane of diffuse scattering for the original crystal. A rich diffuse scattering intensity distribution can be observed, similar to that of pure BNT.^{10,13} L-shaped sharp streaks leading toward lower q-values emanate from the Bragg peaks. Such streaks have been previously observed in pure BNT and have been successfully modeled using planar structures of highly correlated Bi atomic positions, analogous to GPZs,^{10,11} in which an atomic size effect draws the scattered intensity distribution toward lower q-values. Figure 1(b) shows the (hk0) plane while an electric field of 4.6 kV/mm is applied to the crystal in the vertical, (k), direction. Throughout the plane, diffuse intensities are sharpened around the Bragg peaks, however, the broader intensities remain similar in nature. The general sharpening is likely caused by changes in the domain structure, which reduces the width of the diffuse features. Interestingly, the L-shaped scattering associated with the GPZ-type features has reduced. Each of these features are highlighted in Fig. 1(c), which shows a difference map of the initial minus high-field diffuse scattering intensities. The reduction in sharp streaking features is then further evidenced in Fig. 1(d) as a line scan along the (0.7 k 0) direction. This direction is chosen as it does not cross any expected superlattice position. The observed change in the GPZ-type structure under electric field is similar to the response of these features in pure BNT under external pressure,¹⁰ where they are completely removed at 3.7 GPa.

^{a)}Author to whom correspondence should be addressed. Electronic mail: j.daniels@unsw.edu.au.

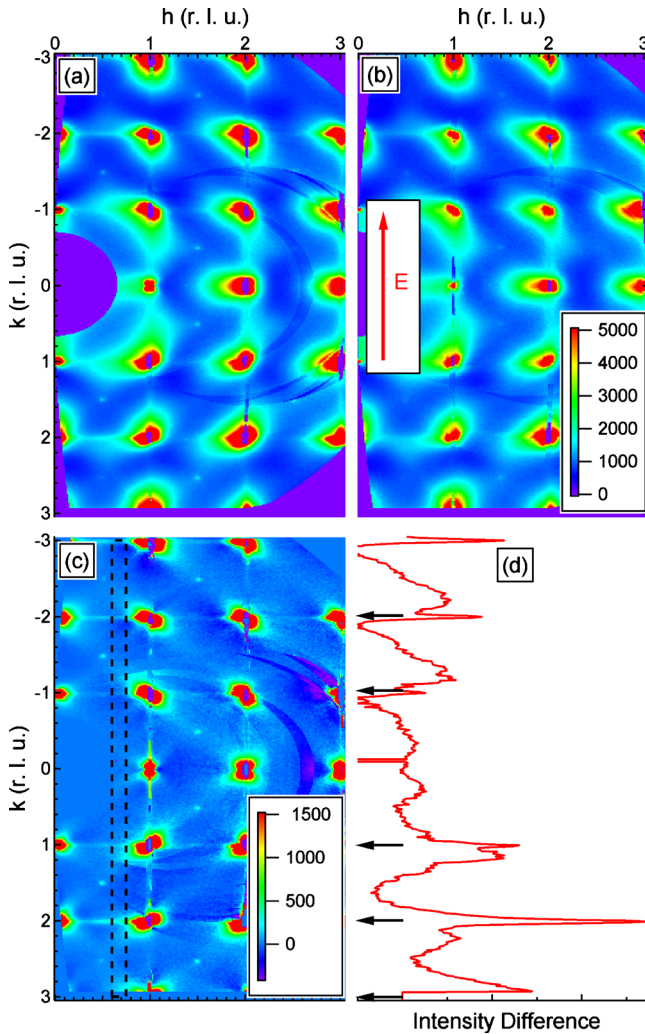


FIG. 1. (Color online) $(hk0)$ reciprocal lattice plane for (a) original state and (b) with an applied field of 4.6 kV/mm in the vertical direction. (c) shows a difference plot of (a) minus (b), which highlights the changes. A line scan at $(0.7 k 0)$ [dashed box in (c)] is shown in (d).

Figure 2(a) shows the $(h k 0.5)$ plane of the initial crystal. Superlattice reflections at the $1/2(00o)$ positions (where o and e are odd and even Miller indices, respectively) are clearly visible; these half-order reflections can be associated with an octahedral tilt system ($a^-a^-a^-$) (Glazer notation¹⁴) that doubles the unit cell in all directions. From the observation of this tilt system it is concluded that this structure has long-range space group symmetry of $R3c$.⁷ Importantly, however, the initial structure shows significant streaking of the superlattice reflections along $\langle 100 \rangle$ directions. This streaking is also seen in Fig. 1(a) cutting through the $(hk0)$ plane at the $1/2(hk)$ positions. Streaking in reciprocal space is commonly attributed to planar defects.¹¹ In the case of these half-order reflections, it would be a stacking fault of two successive tilt systems. Therefore, the observed streaking is consistent with the notion that very fine nanoscale domains of opposing octahedral tilts exist within the single crystal, and that they are separated by a region of different symmetry.¹⁵ It should be noted that the nanoregions observed here are not analogous to those in the relaxor ferroelectric systems of $\text{PbZn}_{1/3}\text{Nb}_{2/3}\text{O}_3\text{-PbTiO}_3$ (PZN-PT) and $\text{PbMg}_{1/3}\text{Nb}_{2/3}\text{O}_3\text{-PbTiO}_3$ (PMN-PT).¹⁶ PZN-PT and PMN-PT show diffuse Bragg peak streaking along $\langle 110 \rangle$ di-

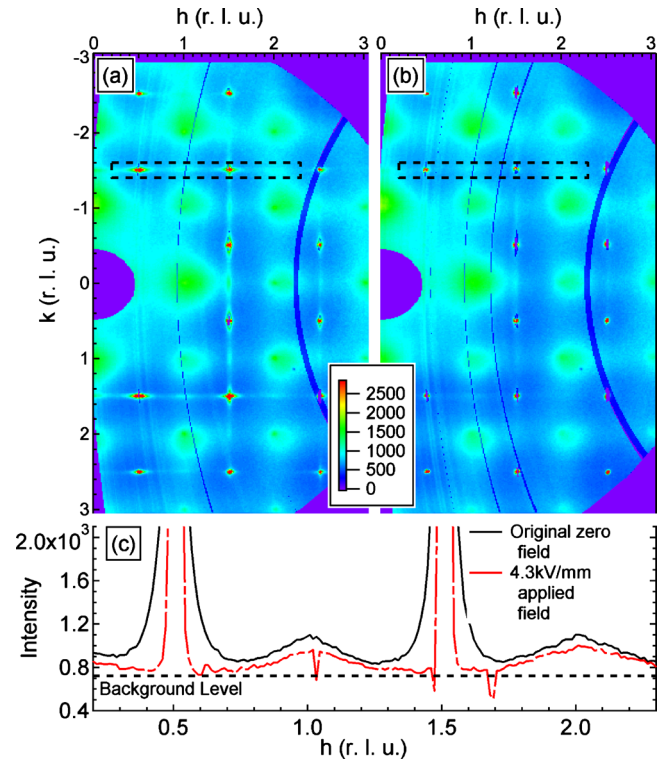


FIG. 2. (Color online) $(h k 0.5)$ planes of diffuse scattering for, (a) initial crystal and (b) an applied electric field of 4.6 kV/mm. (c) shows line scans along the $(h1.50.5)$ direction taken from the areas outlined by dashed boxes in (a) and (b). The estimated background intensity level is indicated in (c).

rections, which have been attributed to plateletlike PNRs, which redistribute under electric field but do not change in volume.¹⁷ The difference in the diffuse features of the two systems originates in the nature of the polarization; the polarization of the lead-containing materials is accompanied by a distortion of the unit cell and subsequent domain formation, whereas the polarization in BNT-BT occurs together with octahedral tilts that double the unit cell. Therefore, diffuse streaking due to the nanoregions in BNT-BT shows up at half order reflections.

Figure 2(b) shows the same $(h k 0.5)$ plane as Fig. 2(a) with an applied electric field of 4.3 kV/mm. The observed streaking between superlattice reflections along $\langle 100 \rangle$ directions is dramatically reduced with the $1/2(00o)$ Bragg spots sharper. This change is highlighted in Fig. 2(c), which shows line scans along the $(h 1.5 0.5)$ direction for both the initial state and with a field of 4.3 kV/mm. Here, the indicated background level is determined from observing intensity at positions in reciprocal space away from any scattering features. The streak intensity can subsequently be measured with respect to this background level. It can be seen that in the initial state, the streak intensity at $k=0.6-0.7$, for example, is well above the general background level. Upon application of the electric field, however, the streak intensity falls to the background level.

The widths of the $(1.5 1.5 0.5)$ reflections shown in Fig. 2(c) have been determined by fitting a pseudo-Voigt peak shape function. The full width at half maximum was determined to be 0.037 and 0.019 reciprocal lattice spacings for the initial and field-on structures, respectively. These widths are inversely correlated with the modulation length of the stacking fault structure. If we assume that the peak width in

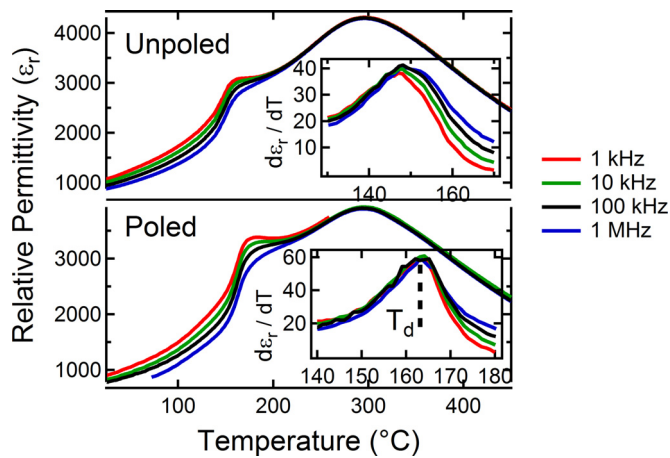


FIG. 3. (Color online) Temperature-dependent permittivity of the unpoled and the poled BNT-4BT single crystal sample. Note the frequency dispersion. The insets are the derivative of the permittivity with respect to temperature.

the field-on measurement is resolution limited, this allows us to calculate a minimum correlation length for the initial structure using a Scherrer-type relation.¹⁸ In this case, we find a minimum correlation length of approximately 20 nm. It should be noted, however, that this does not account for the possibility of a distribution of modulation lengths, which may be caused by a random stacking fault structure.

The measurements presented here are consistent with the structural model proposed by Dorcet and Trolliard.¹⁵ In this model, R3c rhombohedral domains are separated by a stacking fault in which the fault layer has a tetragonal symmetry, where the A-site cation is offset along the $[001]_T$ axis. It is clear that the diffuse scattering associated with the GPZ-type features from the study of Kreisel *et al.*¹⁰ are directly related with the behavior of the stacking fault structure. This is evidenced by the correlated reduction in intensity of both features upon application of electric field.

In order to link the local correlations to the macroscopic electrical properties, we measured the relative dielectric permittivity of the BNT-4BT single crystal in the as-grown unpoled state, and after poling. The growth of the rhombohedral nanoregions during the poling process, and removal of the planar stacking faults as described above, should manifest themselves in the dielectric permittivity of the sample. In PMN relaxors, the frequency-dispersion is believed to come from a thermal evolution of the relaxation time distribution of PNRs generating a random-field at a local scale.¹⁹ The nanoscale structures of the BNT-4BT sample studied here, and those observed in pure BNT, however, are not analogous to those of PMN. Dorcet and Trolliard¹⁵ suggest that the relaxation process in pure BNT cannot be attributed to the nanoscale tetragonal platelets because of a restricted degree of freedom for the A-cation displacements.

Figures 3(a) and 3(b) shows the temperature dependence of the dielectric permittivities measured between 1 kHz and 1 MHz. In both cases, a general frequency-dispersion is clearly visible, showing that BNT-4BT is indeed a relaxor below 200 °C. To highlight the changes in the relative permittivity behavior upon poling, the derivative of the data around the initial inflection point are shown as insets. In the unpoled sample, the temperature of the inflection point in-

creases with frequency. After poling, the point of inflection is consolidated to a single temperature. The frequency-independent inflection point that represents T_d (Refs. 20 and 21) indicates electrical poling induces a sizable macroscopic ferroelectric order in the system.

These results show that BNT-4BT contains short-range structural correlations at the atomic scale and nanometer sized rhombohedral octahedral tilt domains, which are separated by a planar stacking fault, likely of tetragonal symmetry. Application of an electric field of 4.6 kV/mm along a $[100]$ direction removes stacking faults from the crystal and results in growth of the rhombohedral domains. Poling also changes the behavior of the frequency-dependent relative permittivity causing the consolidation of T_d to a single temperature. This shows conclusively that the removal of the tetragonal platelets of the stacking fault plane and the growth of the rhombohedral domains changes the relaxor behavior of BNT-4BT. However, it also shows that general frequency dependence in the relative permittivity at low temperatures remains, regardless of these changes to the nanoscale domain structure, suggesting another contribution to the relaxor behavior in BNT based materials exists.

The European Synchrotron Radiation Facility is acknowledged for provision of x-ray beamtime. J.E.D. acknowledges financial support through an Australian Institute of Nuclear Science and Engineering. This work was carried out under the SFB 595 “Fatigue in functional electrical materials.”

¹J. Rödel, W. Jo, K. Seifert, E.-M. Anton, T. Granzow, and D. Damjanovic, *J. Am. Ceram. Soc.* **92**, 1153 (2009).

²T. Takenaka, K. Maruyama, and K. Sakata, *Jpn. J. Appl. Phys., Part 1* **30**, 2236 (1991).

³C. Ma and X. Tan, *Solid State Commun.* **150**, 1497 (2010).

⁴W. Jo, J. E. Daniels, J. L. Jones, X. Tan, P. A. Thomas, D. Damjanovic, and J. Rödel, *J. Appl. Phys.* **109**, 014110 (2011).

⁵V. A. Isupov, *Ferroelectrics* **315**, 123 (2005).

⁶B. Wylie-van Eerd, D. Damjanovic, N. Klein, N. Setter, and J. Trodahl, *Phys. Rev. B* **82**, 104112 (2010).

⁷G. O. Jones and P. A. Thomas, *Acta Crystallogr., Sect. B: Struct. Sci.* **58**, 168 (2002).

⁸L. A. Schmitt, M. Hinterstein, H. J. Kleebe, and H. Fuess, *J. Appl. Crystallogr.* **43**, 805 (2010).

⁹J. Kling, X. L. Tan, W. Jo, H. J. Kleebe, H. Fuess, and J. Rödel, *J. Am. Ceram. Soc.* **93**, 2452 (2010).

¹⁰J. Kreisel, P. Bouvier, B. Dkhil, P. A. Thomas, A. M. Glazer, T. R. Welberry, B. Chaabane, and M. Mezouar, *Phys. Rev. B* **68**, 014113 (2003).

¹¹T. R. Welberry, *Diffuse X-Ray Scattering and Models of Disorder* (Oxford University Press, New York, 2004).

¹²J. E. Daniels, A. Pramanick, and J. L. Jones, *IEEE Trans. Ultrason. Ferroelectr. Freq. Control* **56**, 1539 (2009).

¹³P. A. Thomas, S. Trujillo, M. Boudard, S. Gorfman, and J. Kreisel, *Solid State Sci.* **12**, 311 (2010).

¹⁴A. M. Glazer, *Acta Crystallogr., Sect. A: Cryst. Phys., Diffr., Theor. Gen. Crystallogr.* **31**, 756 (1975).

¹⁵V. Dorcet and G. Trolliard, *Acta Mater.* **56**, 1753 (2008).

¹⁶G. Xu, Z. Zhong, H. Hiraka, and G. Shirane, *Phys. Rev. B* **70**, 174109 (2004).

¹⁷G. Xu, Z. Zhong, Y. Bing, Y.-G. Ye, and G. Shirane, *Nature Mater.* **5**, 134 (2006).

¹⁸J. I. Langford and A. J. C. Wilson, *J. Appl. Crystallogr.* **11**, 102 (1978).

¹⁹V. Westphal, W. Kleemann, and M. D. Giinckel, *Phys. Rev. Lett.* **68**, 847 (1992).

²⁰K. Datta, P. A. Thomas, and K. Rödel, *Phys. Rev. B* **82**, 224105 (2010).

²¹H. Schremmer, W. Kleemann, and D. Rytz, *Phys. Rev. Lett.* **62**, 1896 (1989).